An Integral Equation Theory of Polymer Blends: Athermal Mixtures†

John G. Curro* and Kenneth S. Schweizer

Sandia National Laboratories, Albuquerque, New Mexico 87185. *Received July 17, 1989*

ABSTRACT: In order to understand the effects of molecular structure on the miscibility of polymer blends, we applied our polymer RISM theory to various athermal mixtures. For the case of athermal blends involving differences in local structure in the components, we obtained an analytical approximation for the generalized Flory–Huggins χ parameter in terms of composition, density, and the molecular parameters monomer size, stiffness, and aspect ratio. Numerical calculations were performed for two "topological blends" involving differences in molecular structure on global length scales: the bimodal mixture and the chain/ring mixture. In contrast to the mean-field, Flory–Huggins theory for which χ is zero, we found that structural asymmetry in the polymer components leads to a negative χ parameter with an approximate linear composition dependence. Both local structure disparities, on a monomer scale, as well as global asymmetry on a radius of gyration length scale lead to significant noncombinatorial entropy of mixing effects. Furthermore, we find that this noncombinatorial entropy of mixing, which stabilizes the miscible mixture, increases when the structural asymmetry is increased. This stabilization is caused by spatially nonrandom packing, which is enhanced by structural differences. Our theory was also used to calculate the total and partial structure factors for athermal mixtures, and comparisons are made with the RPA theory. We find that the RPA theory becomes a poorer approximation when fluctuations in total density increase relative to concentration fluctuations. We also find that in some cases the generalized χ parameter is weakly dependent on wavevector.

Introduction

There has been significant interest in the literature in recent years in the study of polymer mixtures. This is due not only to the technological importance of polymer blends but also to the fact that small-angle neutron scattering (SANS) has led to new insights into the molecular factors that control miscibility in polymer mixtures.[1,2] According to the well-known Flory–Huggins theory,[3] polymer mixtures differ from small molecular weight liquids in that their combinatorial entropy of mixing per monomer, which is negative and hence favors miscibility, is much less important and approaches zero in the infinite chain limit. As a result, the conventional point of view is that specific attractive interactions between unlike polymers are required in order to obtain miscibility in chain molecular liquids at high molecular weight.[4] This point of view has been brought into question, however, as a result of recent studies on polymer blends, which reveal a surprising degree of miscibility, despite the fact that there is no obvious source of specific attractive interactions.[4-7] The purpose of the present investigation is to show that the inclusion of off-lattice effects and concentration fluctuations, not included in the Flory–Huggins theory, tends to stabilize the miscible mixture without invoking specific interactions.

Recently, the present authors developed a new theoretical approach to the study of polymer liquids.[9-14] This theory is based on the "reference interaction site model" (RISM theory) of Chandler and Andersen,[15,16] which has been successful in describing the structure of small molecule liquids. We have also generalized our theory to the case of polymer mixtures.[17-19] Although the theory is quite general, in the present investigation, we apply this polymer RISM theory to the case of the athermal mixture, in which there is no net attraction between monomer units along the chains. In such a mixture, the free energy of mixing is entirely due to entropy of mixing effects. As a result, this will allow us to isolate the effects of molecular structure and chain architecture on polymer miscibility.

A key quantity in the Flory–Huggins theory is the well-known χ parameter,[3,4] which is defined in terms of the nearest-neighbor exchange interaction between monomers. On the basis of this definition, one would expect that $\chi \sim T^{-1}$. It is well-known from experiment, however, that the χ parameter depends on variables such as composition, density, molecular weight, chemical structure,[1,2,5-8] and even wavevector.[31] In our polymer RISM theory, we have shown[17-19] that the χ parameter should be interpreted, not in terms of "bare" attractive interactions as in the Flory–Huggins theory, but in terms of the corresponding "direct correlation functions". In this paper we will denote the Flory–Huggins χ parameter based on the bare attractive interactions as χ_o, in order to distinguish it from our more generalized interpretation. Since this bare χ parameter, χ_o, is by definition energetic in origin, it is identically zero for athermal mixtures. In contrast, our theory predicts a nonzero, structurally dependent χ parameter for athermal blends. In this paper we examine the effect of molecular structure asymmetries between monomers on the χ parameter for the case of binary, athermal mixtures. In particular, we will numerically study blends exhibiting *local* structural asymmetry on the monomeric length scale due to monomers of different size and of different stiffness. In the case of athermal blends exhibiting local structural asymmetries, we are also able to develop an analytical approximation for χ using a continuum limit model. In addition, we also examine "topological blends" exhibiting *global* structure asymmetry on the radius of gyration length scale. The examples we have studied include the bimodal molecular weight blend and the chain/ring mixture. In this paper we will show how these asymmetries in molecular structure affect the miscibility of polymer blends. Furthermore, we will demonstrate that molecular asymmetries between polymers in a binary, athermal blend lead to significant nonrandom mixing effects on all length scales. These concentration fluctuations lead to a rich

† This work performed at Sandia National Laboratories supported by the U.S. Department of Energy under Contract No. DE-AC04-76DP00789.

0024-9297/90/2223-1402$02.50/0

dependence of miscibility on structure totally absent in the classical Flory–Huggins theory.

Theory

The Flory–Huggins lattice theory leads to the following well-known result for the Helmholtz free energy of mixing per monomer for the case of a binary polymer blend[3]

$$\frac{\Delta A}{k_B T} = \frac{\phi \ln \phi}{N_A} + \frac{(1-\phi)\ln(1-\phi)}{N_B} + \chi_o \phi(1-\phi) \quad (1)$$

where ϕ is the volume fraction of monomers of type A, and N represents the degree of polymerization of A or B type monomers. Note that the combinatorial entropy terms become vanishingly small for large N_A and N_B, and thus the Flory–Huggins χ parameter, χ_o, must be negative in order to ensure miscibility for long chains. In the Flory–Huggins picture, χ_o is defined in terms of the bare, nearest-neighbor, attractive energies between monomers, ϵ_{AA}, etc.

$$\chi_o = -(z-2)(\epsilon_{AA} + \epsilon_{BB} - 2\epsilon_{AB})/2k_B T \quad (2)$$

where z is the coordination number of the lattice. It can be seen from eq 2 that, for the athermal mixture, in which there is no net attraction between monomers, the Flory–Huggins χ parameter is identically zero. The Flory–Huggins theory is known to suffer from a number of serious deficiencies, which include the fact that it is an incompressible, lattice model, in which all correlations in concentration and chain connectivity have been essentially ignored. It should be mentioned that Freed and co-workers[20–22] have used field theoretic techniques to *perturbatively* calculate concentration fluctuation corrections to the Flory–Huggins *lattice* model.

We have recently developed an off-lattice, nonperturbative theory for the structure and thermodynamics of polymer liquids.[9–13] This theory, which is an extension to polymers of the RISM theory[15,16] of liquids, was shown[14] to work well for homopolymers when compared with molecular dynamics simulations of chain molecules at liquid-like densities. This polymer RISM theory can be extended to polymer blends[17–19] in a straightforward manner. As in the case of long-chain homopolymers, it is a good approximation to neglect chain-end effects. For the case of the binary blend of two homopolymers, there are three independent, *inter*molecular radial distribution functions $\{g_{AA}(r), g_{BB}(r), g_{AB}(r)\}$ between sites on different chains. We also introduce the *intra*molecular distribution functions $\{\omega_A(r), \omega_B(r)\}$ defined according to

$$\omega_M(r) = N^{-1}\sum_{ij} \omega_{ij}(r; M) \quad (3)$$

where $\omega_{ij}(r; M)$ is the probability that a pair of sites i and j on a single chain of type M are separated by a distance r. The subscripts M or M' refer to the chain type, i.e., component A or B. Following the RISM theory, the corresponding *inter*molecular "direct correlation functions", $\{C_{AA}(r), C_{BB}(r), C_{AB}(r)\}$, are defined according to the three coupled Ornstein–Zernike equations[19]

$$\hat{\mathbf{H}}(k) = \hat{\Omega}(k)\cdot\hat{\mathbf{C}}(k)\cdot[\hat{\Omega}(k) + \hat{\mathbf{H}}(k)] \quad (4a)$$

written for convenience in matrix form where the caret denotes Fourier transformation with wavevector k. The symmetric 2×2 matrices $\mathbf{H}(r)$ and $\Omega(r)$ are defined as

$$\mathbf{H}_{MM'}(r) = \rho_M \rho_{M'}[g_{MM'}(r) - 1]$$
$$\Omega_{MM'}(r) = \rho_M \omega_M(r)\, \delta_{MM'} \quad (4b)$$

$\mathbf{C}(r)$ is the corresponding direct correlation function matrix and ρ_M is the monomeric or site density for species A or B.

As in the case of the homopolymer liquid, for intuitive purposes the direct correlation functions can be thought of as an effective pair potential between intermolecular sites, renormalized by many-body structural effects.[16] In order to have a solvable problem, we take advantage of the fact that the direct correlation function $C_{MM'}(r)$ is a short-range function of intersite spacing r and make use of the Percus–Yevick mean spherical approximation[15,19]

$$H_{MM'}(r) = -\rho_M \rho_{M'} \qquad r < d_{MM'}$$
$$C_{MM'}(r) = -v_{MM'}(r)/k_B T \qquad r > d_{MM'} \quad (5)$$

where $d_{MM'}$ is the hard sphere distance of closest approach between monomers of type M and M', and $v_{MM'}(r)$ is an attractive potential defined for $r > d_{MM'}$. For the athermal case considered in this paper, $v_{MM'}(r)$ is identically zero. The Ornstein–Zernike equations in eq 4 plus the closure relations in eq 5 lead to a set of three, nonlinear integral equations for the radial distribution functions $g_{AA}(r)$, $g_{BB}(r)$, and $g_{AB}(r)$. In general one would expect that the *inter*molecular correlations $g_{MM'}(r)$ and the *intra*molecular correlations $\omega_A(r)$ and $\omega_B(r)$ would have to be solved self-consistently. We circumvent this problem to first order by making use of Flory's conjecture[23] that the intramolecular structure of a chain in a melt is ideal; i.e., long-range excluded-volume interactions are screened out. There is significant neutron scattering and computer simulation evidence to support the accuracy of this conjecture in the homopolymer melt, and this has been discussed previously.[9–14] The accuracy of the ideality assumption in polymer mixtures is, of course, more speculative.[19]

In order to make a connection with SANS experiments, we can also calculate dimensionless, "partial" structure factors defined as[19]

$$\hat{S}_{MM'}(k) = (K_{MM'}/8\pi^3)\int \langle \delta\rho_M(r_1)\delta\rho_{M'}(r_2)\rangle \exp(i\vec{k}\cdot\vec{r}_{12})\, d\vec{r}_{12}$$
$$K_{MM'} = \bar{v}_M \bar{v}_{M'}/\eta(\bar{v}_A \bar{v}_B)^{1/2} \quad (6)$$

where v_M is the average monomer volume for component A or B, η is the packing fraction

$$\eta = \rho_A \bar{v}_A + \rho_B \bar{v}_B$$

and $\delta\rho_M(r)$ is the density fluctuation, $\rho_M(r) - \rho_M$. From the Ornstein–Zernike equations in eq 4, it is possible to show that these partial structure factors can be written as[19]

$$\hat{S}_{AA}(k) = K_{AA}\rho_A \hat{\omega}_A(1 - \rho_B \hat{\omega}_B \hat{C}_{BB})/\hat{\Lambda}$$
$$\hat{S}_{BB}(k) = K_{BB}\rho_B \hat{\omega}_B(1 - \rho_A \hat{\omega}_A \hat{C}_{AA})/\hat{\Lambda}$$
$$\hat{S}_{AB}(k) = K_{AB}\rho_A \rho_B \hat{\omega}_A \hat{\omega}_B \hat{C}_{AB}/\hat{\Lambda} \quad (7)$$

where the denominator is given by

$$\hat{\Lambda}(k) = 1 - \rho_A \hat{\omega}_A \hat{C}_{AA} - \rho_B \hat{\omega}_B \hat{C}_{BB} + \rho_A \rho_B \hat{\omega}_A \hat{\omega}_B (\hat{C}_{AA}\hat{C}_{BB} - \hat{C}_{AB}^2) \quad (8)$$

These partial structure factors, which probe the concentration (volume fraction) fluctuations, can be calculated once the RISM equations have been solved for the direct correlation functions in Fourier space. We can also define a *total* structure factor, $\hat{S}(k)$, which is proportional to

the total specific volume fluctuations.[19]

$$\hat{S}(k) = \hat{S}_{AA}(k) + \hat{S}_{BB}(k) + 2\hat{S}_{AB}(k) \quad (9)$$

For a hypothetical incompressible system, there is only one independent structure factor, $\hat{S}_{AA}(k) = \hat{S}_{BB}(k) = -\hat{S}_{AB}(k)$, and the total structure factor, $\hat{S}(k)$, is zero.

de Gennes has derived[24] the well-known RPA expression for the partial structure factor based on the Flory–Huggins free energy. Our structure factors in eq 7, on the other hand, are considerably more complicated than the RPA equation. We have shown previously,[17,19] however, that if we impose an incompressibility constraint on our theory, we recover the RPA equation (suitably generalized for the case of unequal monomer size)

$$\frac{1}{\hat{S}_{RPA}(k)} = \frac{1}{R^{1/2}\phi\hat{\omega}_A(k)} + \frac{R^{1/2}}{(1-\phi)\hat{\omega}_B(k)} - 2\chi_s \quad (10)$$

where $\hat{S}_{RPA} = \hat{S}_{AA} = \hat{S}_{BB}$ and R reflects the difference in average monomer size; $R = \bar{v}_A/\bar{v}_B$. Furthermore, we are able to identify a generalized χ parameter having the form[19]

$$2\chi_s(k) = \frac{\rho}{[R^{-1/2}\phi + R^{1/2}(1-\phi)]}[R^{-1}\hat{C}_{AA}(k) + R\hat{C}_{BB}(k) - 2\hat{C}_{AB}(k)] \quad (11)$$

where the subscript "s" emphasizes that χ_s refers to scattering rather than thermodynamic experiments, and ρ is the total monomeric density. When χ depends on composition, the thermodynamic and scattering χ parameters are not equal but are related by derivatives with respect to composition.[19] It can be seen from eq 11 that, in general, we find that the χ parameter is wavevector dependent; however, for most purposes, where we are interested in long-wavelength properties, we can take the limit of $k \to 0$. Note the striking similarity of our generalized χ parameter χ_s and the Flory–Huggins definition for χ_o in eq 2. In our generalized χ parameter, the bare attractive interactions, ϵ_{AA}, etc., are replaced by the corresponding zero wavevector part of the direct correlation functions, $\hat{C}(0)$. This fits with the intuitive notion that the direct correlation functions play the role of effective pair interactions, which reflect many-body correlational effects. We can, therefore, calculate χ for any chain model by solving the RISM equations. Unlike the Flory–Huggins case, our generalized χ parameter will depend on composition, molecular weight, and molecular structure.

In this initial work on athermal mixtures we will use an ideal Gaussian model for each of the polymer components in order to calculate[12] the intramolecular structure factors $\hat{\omega}_A(k)$ and $\hat{\omega}_B(k)$. From eq 3 using a Gaussian distribution between intramolecular sites, we obtain[12] the following result for linear chains

$$\hat{\omega}_M(k) = (1-f_M)^{-2}[1 - f_M^2 - 2N_M^{-1}f_M + 2N_M^{-1}f_M^{N_M+1}]$$
$$f_M = \exp(-k^2\sigma_M^2/6) \quad (12)$$

For Gaussian rings, the summations in eq 3 cannot be performed analytically, and we resort to numerical summation[9,10] in order to compute $\hat{\omega}_M(k)$. For the case of fully flexible chains, the statistical segment lengths, σ_A and σ_B, are taken for simplicity to be equal to the hard-sphere diameters d_{AA} and d_{BB}, respectively. These intramolecular structure factors are then used in the Ornstein–Zernike equations, eq 4. One of the difficulties in using an ideal, Gaussian model is the fact that some unphysical intramolecular overlap can occur.[12] This can be dealt with by explicitly removing overlapping configurations in the computation of $\hat{\omega}_M(k)$, as we have done previously,[12] or to estimate the overlap fraction $\Delta_M(N_M)$,[12] a method which we will employ here. The consequence of this intramolecular overlap is to modify the average monomer volume $\bar{v}_M$ according to

$$\bar{v}_M = (\pi d_{MM}^3/6)(1 - \Delta_M) \quad (13a)$$

where the overlap volume fraction Δ_M can be approximated by pairwise averaging the volume $V_0(r)$ of overlapping hard spheres over the intramolecular distribution.

$$\Delta_M \cong (\pi N_M d_{MM}^3/6)^{-1}\sum_{ij}\int V_0(r)\,\omega_{ij}(r;M)\,d\vec{r} \quad (13b)$$

Equation 13b can be easily expressed in terms of incomplete γ functions for the case of the Gaussian distribution used here[12]

$$\Delta_M(N_M) = 2\pi^{-1/2}N_M^{-1}\sum_{i,j}[\gamma(1.5, b_{ij}) - 1.5b_{ij}^{-1/2}\gamma(2, b_{ij}) + 0.5b_{ij}^{-3/2}\gamma(3, b_{ij})] \quad (13c)$$

where $b_{ij} = 3/2|i-j|$ for linear chains and $3/2[|i-j|(1 - N_M^{-1}|i-j|)]$ for the Gaussian ring polymer. For small N_M the overlap fraction depends on molecular weight, but this dependence saturates above about 2000 chain units for flexible, Gaussian chains, as can be seen from Table II of ref 12.

The RISM equations defined by eqs 4 and 5 lead to a set of three coupled, nonlinear integral equations for the case of the binary mixture. These equations can be solved numerically using the same techniques as for small molecules[25] and homopolymer liquids.[9-15] These techniques, developed by Lowden and Chandler,[25] make use of the fact that the RISM equations are equivalent to a variational principle involving a functional I_{RISM} defined by[19]

$$I_{RISM} = \sum_{MM'}\rho_M\rho_{M'}\hat{C}_{MM'}(0) - (8\pi^3)^{-1}\int\{\mathrm{Tr}\,(\hat{\Omega}\cdot\hat{C}) + \ln[\det(1 - \hat{\Omega}\cdot\hat{C})]\}\,d\vec{k} \quad (14)$$

Functional differentiation of I_{RISM} with respect to each of the direct correlation functions leads to a set of three equations

$$\frac{\delta I_{RISM}}{\delta C_{MM'}(r)} = 0 \qquad r < d_{MM'} \quad (15)$$

Following Lowden and Chandler,[25] we represent the direct correlation functions by a third degree polynomial in r

$$C_{MM'}(r) = \sum_{i=1}^{4} a_i^{MM'}\left(\frac{r - d_{MM'}}{d_{MM'}}\right)^{i-1} \quad (16)$$

valid for $r < d_{MM'}$. Substitution of eq 16 into eq 15 leads to a set of 12 coupled, nonlinear *algebraic* equations for the coefficients $a_i^{MM'}$. These nonlinear equations can be solved using standard numerical techniques.

Local Structural Asymmetry

In our theory of polymer blends outlined above, the polymer molecular structure enters only through the intramolecular structure factors, $\hat{\omega}_A(k)$ and $\hat{\omega}_B(k)$, for each of the components. Any asymmetry in structure which leads to differences in these intramolecular structure factors will lead to concentration correlations and a nonzero χ parameter, even for athermal mixtures. In this paper we will examine the effect of both local and global structural asymmetries on miscibility. In this section we

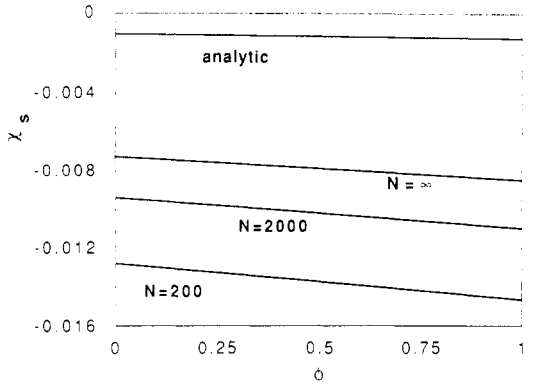

Figure 1. Numerically computed χ parameter as a function of volume fraction of the small component for a binary, tangent hard-sphere blend with $\gamma = 1.2$. The packing fraction is held fixed at 0.45. The curves are at different degrees of polymerization N. The curve labeled "analytic" was computed from eq 28 with $\rho = 1.31$. This "analytic" curve is incorrectly plotted; the correct value of χ is obtained by multiplying the analytic curve by approximately 2.5.

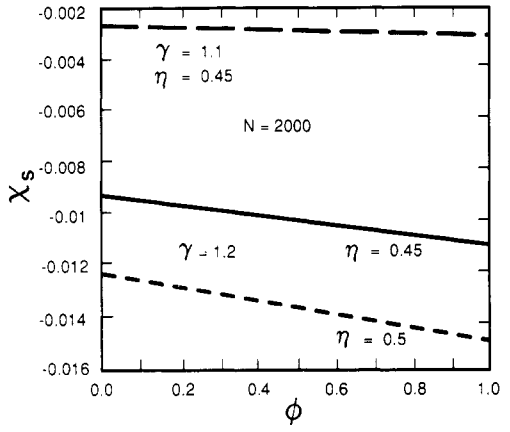

Figure 2. Same as in Figure 1 but for fixed degree of polymerization ($N = 2000$) and several values of the local structural asymmetry parameter, γ, and monomer packing fractions, η.

will focus on local structural effects. At the local or monomeric level we can have differences in structure due to either the monomer size, d_M ($=d_{MM}$), or the statistical segment length, σ_M. The asymmetry in local structure can be specified in terms of three ratios:

$$\gamma \equiv \sigma_B/\sigma_A \qquad \theta \equiv d_B/d_A \qquad \Gamma \equiv \sigma_A/d_A$$

γ is the relative segment length or "stiffness" ratio, θ is the relative segment diameter or "size" ratio, and Γ is the "aspect" ratio, which is a measure of the stiffness of chain A relative to its thickness.

Numerical Results. The simplest athermal mixture is the case for which $\gamma = \theta$, $\Gamma = 1$, and $N_A = N_B = N$. This represents a mixture of fully flexible, tangent hard-sphere, Gaussian chains. The RISM equations, eqs 4 and 5, were solved numerically for this case using the method described above in order to obtain the 12 "a-coefficients" in eq 16. The direct correlation functions, $\hat{C}_{MM'}(0)$, were then computed and used in eq 11 to obtain the generalized χ parameter. The results for the χ parameter of this tangent hard-sphere blend are shown in Figures 1 and 2 as a function of composition.

In the Flory–Huggins theory, χ is zero by definition for all athermal mixtures. In our case, however, it can be seen from Figure 1 that χ is negative and increases with chain length. This chain-length dependence is due to increased "correlation hole" effects,[19] which tend to reduce the direct correlation functions at $k = 0$. It is interesting to note that χ remains negative, even in the infinite chain limit. This implies that there is a noncombinatorial contribution to the entropy of mixing, primarily of local packing origin, which persists for long chains and enhances miscibility. The composition dependence seen in Figure 1 is approximately linear such that χ_s decreases when the volume fraction of the smaller monomer size component is increased. For an asymmetry ratio of $\gamma = 1.2$, the composition dependence is about a 20% effect.

In Figure 2 we examine the effects of total monomeric packing fraction and local structural asymmetry on the χ parameter. We can see from this figure that χ decreases (becomes more negative) as the total packing fraction increases. Again this can be attributed to correlation hole effects, which decrease, thereby resulting in less intramolecular screening and enhanced intermolecular order, as the density increases. We also see in Figure 2 that the χ parameter of the tangent hard-sphere chain blend decreases rather strongly when we increase the asymmetry. This implies that the noncombinatorial entropy of mixing is enhanced when the asymmetry in local structure is increased.

We can obtain insights into the extent of nonrandom packing by examining the individual intermolecular radial distribution functions. We have previously shown[19] that for the tangent hard-sphere blend, the radial distribution functions very nearly obey the simple scaling relations

$$g_{AA}(r/\sigma_{AA}) = g_{BB}(r/\sigma_{BB}) = g_{AB}(r/\sigma_{AB})$$

One measure of the "nonrandomness" of the mixing is given by

$$\Delta g(r) \equiv g_{AA}(r) + g_{BB}(r) - 2g_{AB}(r)$$

Δg is plotted for the tangent hard-sphere mixture in Figure 4. Note that significant positive correlations occur locally and approach zero near the radius of gyration.

Analytical Approximation. For Gaussian, hard-core homopolymer melts we have recently shown[13] that the polymer RISM equation can be solved analytically within a so-called "continuum limit model". Besides the theoretical appeal of an analytic solution, the availability of simple formulas offers qualitative physical insight into the numerical polymer RISM results. In this section, we consider a continuum limit model of a local athermal blend for which the three coupled RISM integral equations can be exactly solved in closed form.

The basic model binary blend of interest consists of ideal Gaussian chains of equal degrees of polymerization, N, component molecular densities ρ_A and ρ_B, statistical segment lengths σ_A and σ_B, and spherical site or segmental diameters d_A and d_B. The continuum limit description of this model blend corresponds to taking the limits $N \to \infty$, $\rho_M \to \infty$, $d_M \to 0$, and $\sigma_M \to 0$, where $M = A, B$. The limiting procedure is done under the restrictions that the total segment density, ρ, is finite. In addition, the continuum limit is performed such that the structural asymmetry ratios γ, θ, and Γ are also finite. In this continuum limit the system can be thought of as consisting of flexible, infinitely thin and long Gaussian "threads" or "strings".

The mathematical virtues of this limiting model are 2-fold. The first simplication is that since the hard-core diameters approach zero, the direct correlation functions "inside the core" for the athermal polymer RISM

theory must be of a δ-function form

$$C_{MM'}(r) = \hat{C}_{MM'}(0)\,\delta(\vec{r}) \equiv C_{MM'}\delta(\vec{r})$$
$$\hat{C}_{MM'}(k) = C_{MM'} \quad \text{for all } k \tag{17}$$

where $C_{MM'}$ are the integrated strengths of the species-dependent direct correlation functions. The second simplification is that since N is diverging and the statistical segment lengths are approaching zero, the "intermediate" wavevector regime, defined as $R_G^{-1} < k < \sigma^{-1}$, expands to cover all values of wavevector. Therefore, the intramolecular structure factors defined by eq 12 reduce to the simple Debye scaling forms:

$$\hat{\omega}_M(k) = 12(k\sigma_M)^{-2} \quad \text{for } M = \text{A, B} \tag{18}$$

Mathematical solution of the athermal binary blend polymer RISM theory (eqs 4 and 5) requires choosing the direct correlations functions such that the intermolecular pair correlations functions vanish inside the hard-core diameter. For the continuum limit model these "core conditions" apply at a single point, i.e.

$$\lim_{r\to 0} g_{MM'}(r) \equiv 0 \tag{19}$$

When eqs 4, 17, and 18 are used, the core conditions of eq 19 can be written as three coupled nonlinear algebraic equations for the direct correlation function *parameters* defined in eq 17. When the dimensionless wavevector variable, $K = k\sigma_A$ is introduced, straightforward analysis yields

$$-1 = 72(\pi^2\sigma_A^3)^{-1}\int_0^\infty [C_{AA}K^2 + 12\rho_B\gamma^{-2}(C_{AB}^2 - C_{AA}C_{BB})]K^{-4}\hat{\Lambda}^{-1}\,dK \tag{20a}$$

$$-1 = 72(\pi^2\sigma_A^3)^{-1}\int_0^\infty [C_{BB}K^2\gamma^{-4} + 12\rho_A\gamma^2(C_{AB}^2 - C_{AA}C_{BB})]K^{-4}\Lambda^{-1}\,dK \tag{20b}$$

$$-1 = 72(\pi^2\sigma_A^3)^{-1}\int_0^\infty K^{-2}C_{AB}\gamma^{-2}\Lambda^{-1}\,dK \tag{20c}$$

where $\hat{\Lambda}(K)$ in eq 8 can be rewritten using eqs 17 and 18 as

$$\hat{\Lambda}(K) = 1 - 12\,(\rho_A C_{AA} + \rho_B C_{BB}\gamma^{-2})K^{-2} - 144\gamma^{-2}\rho_A\rho_B(C_{AB}^2 - C_{AA}C_{BB})K^{-4} \tag{21}$$

Remarkably, these equations are solved by the simple "scaling" relations

$$C_{AA}C_{BB} = C_{AB}^2 \tag{22}$$

$$C_{BB} = \gamma^4 C_{AA} \qquad C_{AB} = \gamma^2 C_{AA} \tag{23}$$

and where C_{AA} is given as the solution of the single transcendental equation:

$$-1 = 72(\pi^2\sigma_A^3)^{-1}\int_0^\infty dK \frac{C_{AA}}{[K^2 - 12(\rho_A + \gamma^2\rho_B)C_{AA}]} \tag{24}$$

Equation 24 is easily solved with the result

$$\rho_A C_{AA} = -\frac{\pi^2}{108}(\rho_A\sigma_A^3)^2\left(1 + \gamma^2\frac{\rho_B}{\rho_A}\right) \tag{25}$$

There are several interesting features of this exact solution: (1) Equation 22 is analogous to a geometric average "combining law", or "Berthelot rule", often employed in the theory of atomic mixtures for the Lennard-Jones *energy* parameters.[26] For the present purely repulsive force blend system, it is the direct correlation function that plays the role of an effective, or renormalized, potential. (2) The "scaling" relations of eq 23 are a direct result of the purely power law intramolecular correlations described by eq 18. (3) The intermolecular pair correlation functions obey the "random mixing" relation: $g_{AA}(r) = g_{AB}(r) = g_{BB}(r) \equiv g(r)$. Therefore, this purely repulsive continuum limit model is structurally "mean-field", in the same way that the infinitely weak, but infintely long-ranged, attractive Kac-potential model[27] is. Nevertheless, the repulsive continuum limit does have nontrivial thermodynamic consequences in the sense that the effective χ parameter is nonzero (see below). (4) The intermolecular pair correlation function, $g(r)$, is of the identical *form* as for the homopolymer melt case,[13] the only difference being the effective screening length. Simple analysis yields the analytic result:

$$\rho_A\sigma_A^3[g(R) - 1] = \frac{-3}{\pi R(1 + \gamma^2\rho_B/\rho_A)}[1 - \exp(-R/\xi)] \tag{26}$$

where

$$R \equiv r/\sigma_A \qquad \xi^{-1} \equiv \frac{\pi}{3}(1 + \gamma^2\rho_B/\rho_A)\rho_A\sigma_A^3$$

The effective χ parameter for the continuum limit blend model is rigorously independent of wavevector and is obtained by substituting eqs 22, 23, and 25 into the general formula given in eq 11. Simple manipulations yield the explicit result:

$$\chi_s = \frac{-\pi^2\rho^2\Gamma^6\theta^{3/2}}{216}(1 - \gamma^2\theta^{-3})^2[\phi + \gamma^2\theta^{-3}(1 - \phi)] \tag{27}$$

The most general features of the effective χ parameter are that it is negative (implying complete miscibility from repulsive forces and structural asymmetries) and a linear function of composition. The latter behavior implies that the corresponding "thermodynamic" χ parameter will also be a linear function of concentration but with a reduced quantitative dependence.[19] Both the absolute magnitude and the size and direction of the composition dependence depend sensitively on the value of the quantity $\gamma^2\theta^{-3}$. This quantity is a ratio of two ratios: the segmental surface area ratio relative to the segmental volume ratio. Equation 27 also predicts that the effective χ parameter becomes more negative with increasing total monomer density and/or aspect ratio, although the relative composition dependence is unaffected by these quantities. Finally, although the present model has assumed ideality and constant volume, deviations from this limit can be incorporated in a "post facto" manner by simply inserting a composition-dependent total density, $\rho(\phi)$, and/or segment length (or equivalently radius of gyration), $\sigma_M(\phi)$, in eq 27 if known experimentally or from independent theoretical calculations.

Comparison with Numerical RISM Calculations. The numerical calculations presented in the preceding section were for finite length and nonzero thickness Gaussian, tangent hard-sphere chains characterized by equal statistical segment length and hard-core diameters; i.e., $\sigma_M = d_M$. In order to access the realism and limitations of the analytic continuum limit model, it is of interest to compare its predictions with the exact numerical RISM results. For the case studied numerically ($\theta = \gamma$ and $\Gamma = 1$) the analytic result becomes

$$\chi_s = \frac{-\pi^2\rho^2\gamma^{-1/2}}{216}(\gamma - 1)^2[\phi + (1 - \phi)/\gamma] \tag{28}$$

The qualitative prediction of a negative, linearly concentration-dependent χ parameter, which becomes more negative with increasing small monomer species volume frac-

tion, is in excellent agreement with the numerical results of Figures 1 and 2.

To quantitatively compare predictions of *relative* trends, we consider the $N = 2000$ calculations of Figures 1 and 2. To compare the dependence of χ on the structural asymmetry parameter, γ, note that for $\phi = 0.5$ the continuum model predicts that the absolute magnitude of χ increases by the factor of 3.68 when γ is increased from 1.1 to 1.2. The numerical RISM calculations for a total effective packing fraction of 0.45 (corresponding to a $\rho = 1.31$) yield a factor of 3.67 increase, in exact agreement with the analytic model! The numerical results for the structural asymmetry dependence of χ are virtually independent of density ρ at high densities, in agreement with eq 28. The magnitude of the (linear) composition dependence predicted by the analytic model is simply given by $\chi_s(\phi = 1)/\chi_s(0) = \gamma$. From Figure 2 the numerical calculations yield for this ratio 1.093 (for $\gamma = 1.1$) and 1.188 (for $\gamma = 1.2$), which agree with the continuum model predictions to within 10%. We have also found that the magnitude of the composition dependence of χ as calculated numerically is a very weakly increasing function of density, again in excellent agreement with eq 28. At fixed 50% volume fraction composition and a $\gamma = 1.2$, the numerical RISM calculations show that χ increases in absolute magnitude by a factor of 1.33 when the packing fraction is increased from 0.45 to 0.5 (density increased from $\rho = 1.331$ to 1.479). The corresponding continuum model prediction is a factor of 1.235 increase, which is somewhat weaker. The underestimation by the analytic model of the density dependence of χ is consistent with our previous findings[13] for the homopolymer Gaussian melt and is easily understandable as a natural quantitative limitation of continuum type models. Finally, one can compare the absolute magnitude of χ predicted by the analytic model relative to the numerically determined, extrapolated $N \rightarrow \infty$ result for $\phi = 0.5$ and $\gamma = 1.2$ displayed in Figure 1. As can be seen from this figure, χ from the analytic model is underestimated by a factor of approximately 3. This is again consistent with the quantitative discrepancies found for the homopolymer melt case of ref 13. Thus the analytic continuum model appears to be remarkably accurate for the relative structural asymmetry and composition dependence of χ for Gaussian, athermal blends. A more sophisticated analytical approach, which explicitly accounts in an approximate manner for the nonzero hard-core segmental volume, has also been developed and extensively applied elsewhere.[28]

Special Cases. In addition to the special case discussed above, there are several other limiting regimes of the structural parameters of particular physical interest. Consider first a "monomer size" blend for which the chain "stiffnesses" are identical; i.e., $\gamma = 1$. In this limit, eq 27 becomes

$$\chi_s = \frac{-\pi^2\rho^2\Gamma^6\theta^{3/2}}{216}(1-\theta^{-3})^2[\phi + \theta^{-3}(1-\phi)] \qquad (29)$$

Clearly, the absolute magnitude of χ is a strongly increasing function of the deviation of the monomer volume ratio from unity. χ becomes more negative with increasing volume fraction of the smaller segment species and for $\theta > 1$ is a factor of θ^3 larger in magnitude for the pure smaller segment component limit compared with the neat larger monomer case. A second special case of interest is a "flexibility or stiffness" blend for which the segmental volumes are identical; i.e., $\theta = 1$. In this limit, eq 27 becomes

$$\chi_s = \frac{-\pi^2\rho^2\Gamma^6}{216}(\gamma^2-1)^2[\phi + \gamma^2(1-\phi)] \qquad (30)$$

Interestingly, for this case the composition dependence of χ is in the opposite direction to that for the monomer size blend and is relatively weaker. The effective χ parameter becomes more negative as the volume fraction of the "stiffer" (large σ) component increases. A third interesting case of eq 27 is when the inequality $\gamma^2\theta^{-3} \ll 1$ or $\gg 1$ is obeyed. For this situation the relative composition dependence is very large, although still linear of course. Such a limiting case is realizable physically if, for example, the B-monomer volume is much larger than for the A-monomer *and* the B-species has a smaller statistical segment length. In practice, this may be an unlikely combination unless, possibly, aromatic groups are present along the backbone. Finally, inspection of eq 27 immediately suggests that a truly "ideal" athermal mixture state is possible even if the two blend components differ structurally. That is, if $\gamma^2\theta^{-3} = 1$, then χ is identically zero! This special point can be though of as the local athermal blend analogue of a Boyle or θ point in polymer solutions. Obviously, if $\gamma^2\theta^{-3}$ is very close, but not equal, to unity the effective χ parameter will be very small and nearly composition-independent.

Experimental Application. PMMA/PEO Blends. Using small-angle neutron scattering (SANS), Ito, Russell, and Wignall[6] have recently determined the effective χ parameter of high molecular weight blends of poly(methyl methacrylate) (PMMA) and poly(ethylene oxide) (PEO). Since there are no obvious "specific" interactions between these two polymers, it is somewhat surprising that they found this mixture to be miscible with a negative χ parameter of the order of −0.002 (for 50% PMMA monomer fraction). Moreover, when the temperature was increased from 25 to 80 °C, no change in the measured χ parameter was detected. This implies that miscibility is not associated with favorable attractive intermolecular interactions but rather derives from a stabilizing noncombinatorial entropic contribution to the free energy of mixing. Within the context of the classical Flory–Huggins theory, these observations have no explanation. In addition, the so-called "equation-of-state" or compressibility effects in polymer blends[4b,c] cannot be playing a major role since they always *de*stabilize the mixture, resulting in a *positive* entropic χ parameter. Hence, the miscibility of PMMA and PEO represents an intriguing and unexplained observation.

From our very simple continuum athermal model perspective, an obvious difference between PEO and PMMA is that both their monomer volumes and statistical segment lengths are quite different. Equation 27 predicts a negative, entropic χ parameter contribution which depends sensitively on the quantity $\gamma^2\theta^{-3}$, which can be expressed in terms of experimentally known parameters as

$$\gamma^2\theta^{-3} = (L_B/L_A)^2\frac{C_B^\infty}{C_A^\infty}\frac{\bar{v}_A}{\bar{v}_B} \qquad (31)$$

where L_M is the effective bond length, C_M^∞ is the characteristic ratio, and $\bar{v}_M$ is the monomer volume of species M.[23] The monomer volume for PMMA is 140.4 Å^3 and 65.8 Å^3 for PEO, while the corresponding characteristic ratios are 6.9 (atactic PMMA) and 4.0, respectively.[6] The effective bond length ratio is very close to unity. Using these numbers, an aspect ratio of 1 for PEO and a typical total packing fraction of 0.5, one obtains

the following estimate from eq 27 for a 50% volume fraction blend: $\chi_s = -0.004$. As discussed in the previous subsections, the continuum model is expected to underestimate the absolute magnitide of χ. On the other hand, for a PMMA with a mixture of tacticities one knows that the characteristic ratio increases.[23] A reasonable upper limit is roughly 9, which then yields a χ parameter of approximately -0.0004. These theoretical estimates are qualitatively consistent with the observed values of χ and provide a zeroth-order rational basis for the entropic miscibility of PMMA and PEO. The predicted linear composition dependence is in qualitative agreement with the experimental trend but is *much smaller* in magnitude than observed. Of course, the coarse-grained theoretical model of the polymer structure is very crude and does not take into account the fact that the degrees of polymerization of PMMA and PEO were very different in the experimental system nor the quenched randomness along the PMMA backbone associated with tacticity variations. On general grounds we expect both the latter physical effects to make negative, entropic contributions to the effective χ parameter and also to introduce additionl composition dependence. Whether a realistic accounting for these multiple structural features will explain the observations awaits a detailed numerical theoretical study. It is interesting to note that on the basis of eq 27, we would predict a negative χ and miscibility even in the limit of infinite molecular weight of both species. The molecular weight dependence was not studied, however, by Ito, Russell, and Wignall,[6] and it is possible that equation-of-state effects, not considered here, would force phase separation at sufficiently high molecular weights in this mixture.

Topological Blends

We have seen in the previous sections that asymmetry in local structure, on a monomeric length scale, leads to significant noncombinatorial entropy of mixing effects which favor miscibility. Since the intramolecular structure factors $\hat{\omega}_A(k)$ and $\hat{\omega}_B(k)$ are also sensitive to structure on a radius of gyration length scale, we anticipate that global structural asymmetry will also lead to interesting entropy of mixing effects. We denote blends that exhibit such global asymmetry as topological blends. In this study we examined the miscibility characteristics of two topological blends: the bimodal chain blend and the chain/ring mixture.

Let us first consider the case of an athermal bimodal mixture of Gaussian chains having identical local structure ($\gamma = \theta$, $\Gamma = 1$) but with unequal chain length ($N_A > N_B$) and, of course, unequal radii of gyration ($R_G^2 = N_A\sigma^2/6$ and $N_B\sigma^2/6$). The polymer RISM equations, eqs 4 and 5, were solved using the numerical techniques discussed above with intramolecular structure factors given by eq 12 for Gaussian chains. The results for the χ parameter are shown in Figure 3 as a function of concentration for various ratios N_B/N_A. It can be seen that, like the case of local asymmetry, the bimodal blend exhibits a negative χ parameter with a linear composition dependence. The composition dependence is modest, with χ decreasing from the pure short-chain ($\phi = 0$) to the long-chain ($\phi = 1$) system. Furthermore, χ_s decreases nonlinearly ($-\chi_s \sim [N_A/N_B - 1]^2$) with the relative asymmetry ratio N_A/N_B. The behavior of χ in the limit where both components become large was not studied here. It should be mentioned that although we studied blends differing in molecular weight by as much as a factor of 10, in reality the ideality assumption must break down as the disparity in chain length increases. In order to account for this effect, the intermolecular and intramolecular structure must be solved self-consistently, which is beyond the scope of the present investigation. We do not expect, however, that the nonideality corrections will qualitatively change the present findings.

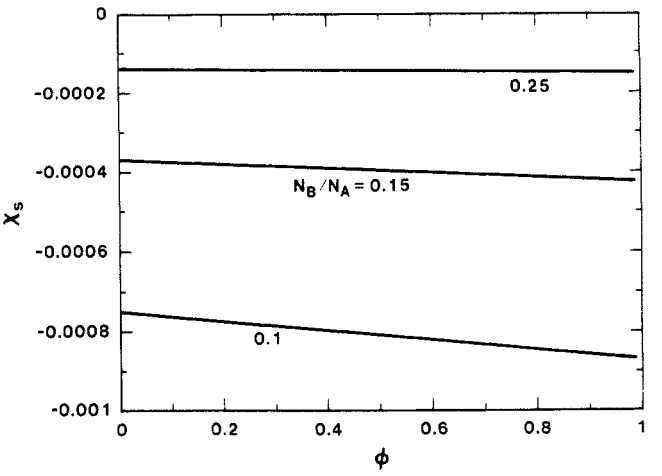

Figure 3. χ parameter calculated for bimodal blends as a function of the volume fraction of component A. The computations are at fixed $N_A = 2000$ and the various values of the ratio N_B/N_A shown on each curve. The packing fraction is held fixed at 0.50.

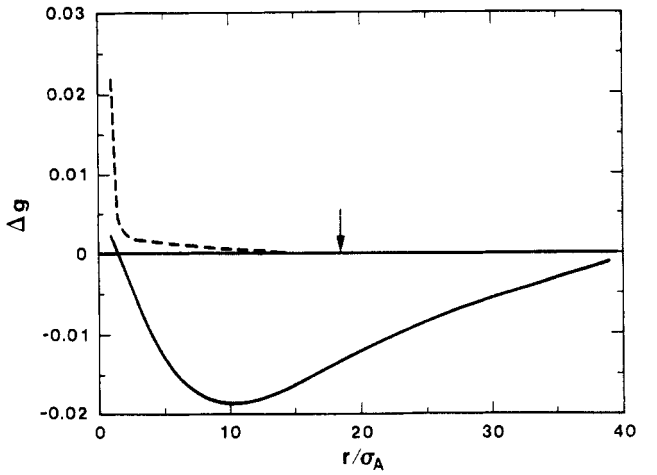

Figure 4. Structural correlation parameter, $\Delta g = g_{AA} + g_{BB} - 2g_{AB}$, as a function of interchain site distance r normalized by the statistical segment length σ_A. For completely random mixing, $\Delta g = 0$. The dashed curve is for the tangent hard-sphere blend as in Figure 1 for $\phi = 0.50$ and $N = 2000$. The solid curve is for the bimodal blend as in Figure 3 for $N_B/N_A = 0.10$ and $\phi = 0.50$. The arrow refers to the radius of gyration of a 2000 unit chain.

Although the χ parameters for the bimodal mixture and the local blends exhibit similar behavior, the structural correlations are quite different. This can be seen in Figure 4 where we compare the nonrandomness of the mixing for the tangent hard sphere and the bimodal mixtures. It can be observed that the structural correlations for the bimodal blend are of opposite sign and much longer range, persisting well beyond the radius of gyration of the long chains. Thus nonrandom mixing is seen on all length scales. This difference in behavior is to be expected since, in contrast to the tangent hard-sphere blend, the bimodal mixture has intramolecular asymmetries on a radius of gyration length scale.

Another topological blend of interest consists of an athermal mixture of linear chains and rings. Considerable interest exists in the literature on chain/ring mixtures from the standpoint of obtaining insights into the dynamics

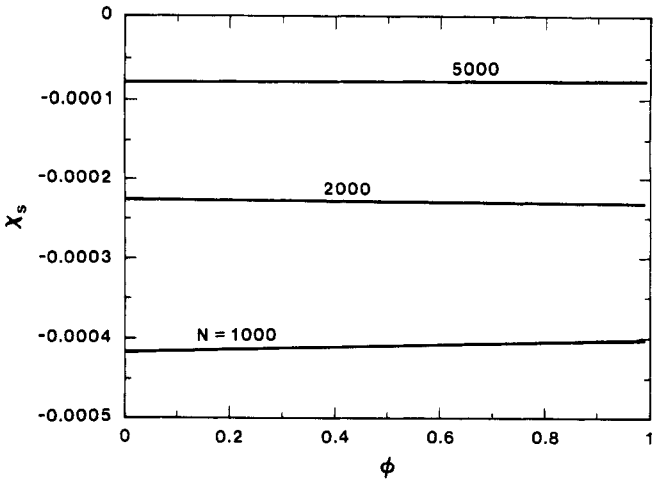

Figure 5. χ parameter calculated for a chain/ring mixture as a function of the volume fraction of linear chains. The computations were performed at equal degrees of polymerization of both species resulting in R_G(chain) = $\sqrt{2}R_G$(ring). The packing fraction was held fixed at 0.50.

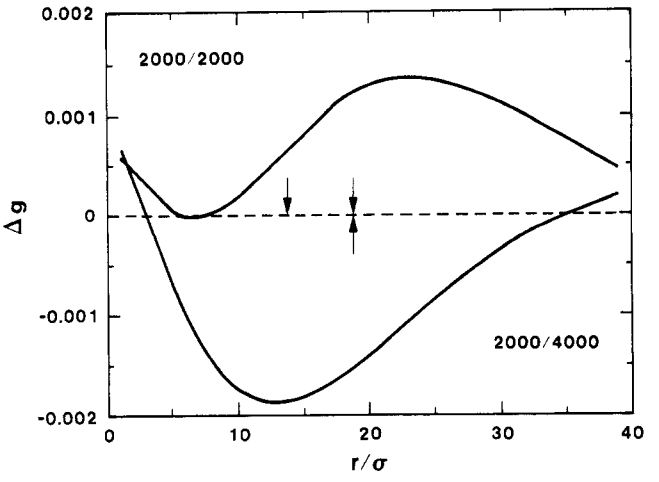

Figure 6. Structural correlation parameter, $\Delta g = g_{AA} + g_{BB} - 2g_{AB}$, as a function of interchain site distance r normalized by the statistical segment length σ. For completely random mixing, $\Delta g = 0$. The upper curve is for $N_A = N_B = 2000$ with R_G = 12.9 (18.3) for the ring (chain) shown by the upper arrows. The lower curve is for a blend of 2000 unit chains and 4000 units rings with R_G = 18.3 for both species shown by the lower arrow. The calculations were performed at fixed ϕ = 0.50 and η = 0.50.

of polymers. Here we will focus on the equilibrium properties and the χ parameter. As in the previous cases we will take the intramolecular structure of the components to be ideal and Gaussian. Justification for this assumption is somewhat tenuous since, to our knowledge, neutron scattering experiments have not yet been performed on polymer ring liquids. Recent computer simulations[29] and intuitive arguments[30] suggest the existence of nonclassical scaling exponents in pure ring liquids. These simulations also suggest that, in mixtures of rings with chains, ideal behavior of both rings and chains exists on long length scales, although some local chain expansion was seen. We consider a chain/ring blend with identical local structure ($\gamma = \theta$, $\Gamma = 1$) in which $\hat{\omega}_A(k)$ is determined by eq 12 for linear chains, and $\hat{\omega}_B(k)$ for the ring is found numerically.[9,10]

Numerical solution of the polymer RISM equations leads to the prediction of a negative χ parameter, implying complete miscibility of chain/ring mixtures. Furthermore, it can be seen from Figure 5 that χ_s is essentially independent of composition for the equal molecular weight blend ($N_A = N_B$). It can also be seen from Figure 5 that χ increases with molecular weight; in fact, we find that $-\chi_s \sim N^{-1}$. Thus, in contrast to the case of the local structural asymmetry blends where χ remains nonzero, χ approaches zero in the infinite chain limit in this topological blend. This is not surprising since the intramolecular structure factors for linear chains and rings approach each other at large N.

The nonrandomness of mixing is shown in Figure 6 where Δg is plotted for both the equal molecular weight mixture ($R_G^2 = N_A\sigma^2/6$ for chains and $N_B\sigma^2/12$ for rings) and the case of $N_A = 2N_B$ (equal radii of gyration). The structural correlations are seen to be 1 order of magnitude smaller in amplitude than the bimodal blend but persist well beyond the largest radius of gyration. It can also be observed from Figure 6 that qualitatively different behavior is seen in Δg depending on whether the radii of gyration are equal or not. In both cases we observe a negative χ parameter since both positive and negative correlations stabilize the miscible mixture.

Discussion and Conclusions

As we have seen, the polymer RISM theory we have developed reduces to the RPA expression for the partial structure factors of the blend when we impose an incompressibility constraint on the system. Our theory does not require this imcompressibility constraint and, therefore, is more general than the RPA theory. It is of interest then to compare the RPA result in eq 10 with the more exact predictions for the partial structure factors from eqs 7 and 8. Such a comparison is shown in Figure 7 for the three athermal blends studied numerically. When plotted as in Figure 7, the RPA expression, which is of the Lorentzian form in the intermediate scaling regime, predicts straight line behavior. The exact structure fac-

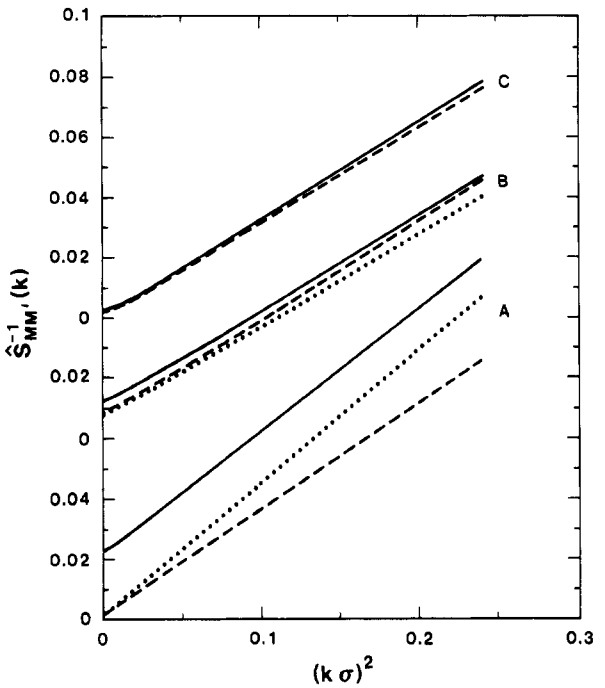

Figure 7. Reciprocal partial structure factors versus $(k\sigma)^2$ for three binary blends: A, tangent hard-sphere mixture, ϕ = 0.50, η = 0.45, $N_A = N_B$ = 2000; B, bimodal blend, ϕ = 0.50, η = 0.50, N_A = 2000, N_B = 200; C, chain/ring mixture, ϕ = 0.50, η = 0.50, $N_A = N_B$ = 2000. Note that the vertical axis has been displaced for clarity for each set of curves. M and M' refer to species of type A or B. The solid lines refer to the RPA predictions, the dashed lines to S_{BB}, and the dotted lines to S_{AA}. For curve A σ is to be interpreted as σ_A.

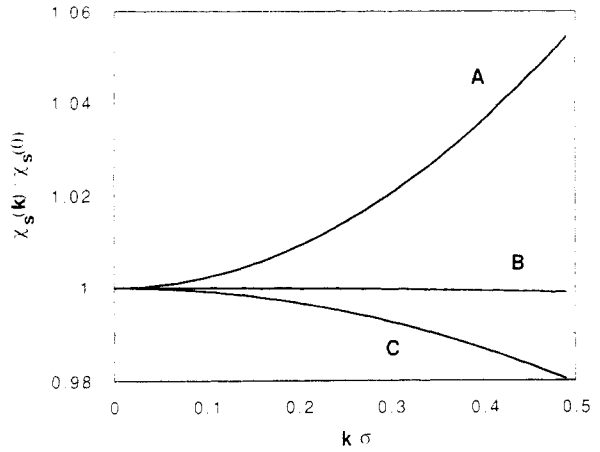

Figure 8. Relative wavevector dependence of the χ parameter for three binary blends. The mixtures A–C are the same as in Figure 7.

tors are also seen to be almost Lorentzian in shape, however, departures can be noticed from the approximate RPA prediction.

Since the RPA formula is exact only in the incompressible limit, we expect that it will become progressively poorer as the total compressibility of the system increases relative to the concentration fluctuations. One measure of the importance of these compressibility effects is given by the ratio $\hat{S}(0)/\hat{S}_{AA}(0)$. For the three blends plotted in Figure 7 this ratio of total density to concentration fluctuations was 0.014 for mixture A (tangent hard-sphere chains), 0.0035 for mixture B (bimodal blend), and 0.0008 for mixture C (chain/ring). As expected the higher the ratio $\hat{S}(0)/\hat{S}_{AA}(0)$, the poorer the RPA theory prediction for the partial structure factors. We have seen that, for athermal mixtures, complete miscibility (negative χ) was predicted in all the cases studied. This implies that the composition fluctuations are small compared to those in mixtures having a positive χ. We anticipate that the $\hat{S}(0)/\hat{S}_{AA}(0)$ ratio will be much smaller in immiscible mixtures, and the RPA theory should be a much better approximation in such systems.

We see from eq 11 that the generalized χ parameter is wavevector dependent through the direct correlation functions. For thermodynamic purposes we are interested in long-wavelength properties; hence, we have taken the zero wavevector limit. For scattering predictions, however, the wavevector dependence of χ may be important. In fact Brereton[31] et al. have proposed that χ must be wavevector dependent in order to explain their SANS data on the poly(tetramethyl carbonate)/deuterated polystyrene blend. In Figure 8 we have plotted the wavevector dependence of χ_s for the same three blends as in Figure 7. It can be seen that for these athermal blends that χ is weakly dependent on k in the intermediate wavevector regime. Furthermore, the sign of the k-dependence is opposite for the local and topological blends. It should be mentioned that the increase of χ_s with wavevector, as found in the local blend of tangent hard-sphere chains, is qualitatively similar to the behavior observed by Brereton and co-workers. Their system was certainly not athermal however.

In the present investigation we have found for athermal mixtures that χ always appears to be negative, which implies complete miscibility of these systems. Furthermore, we find that χ becomes more negative; i.e., the miscible mixture becomes more stable, as the asymmetry in structure (both locally and globally) increases. At first sight this may appear to be counterintuitive; however, it should be recognized that in athermal mixtures the mixing free energy is entirely entropic. Thus structural asymmetry on any length scale increases the packing opportunities of the chain segments leading to nonrandom mixing and noncombinatorial entropy effects. This can be visualized easily for the case of the athermal mixture of hard spheres of different sizes. In this case it is well-known that the small spheres preferentially pack between the large spheres. In the connected polymer chain these nonrandom-packing effects are more subtle but, nevertheless, important. Furthermore, a continuous space theory of the type presented here, as opposed to a lattice description, is much better suited to capture these subtle effects. It, therefore, appears that one possible strategy for "molecularly engineering" miscible polymer blends would be to make the polymers more dissimilar in order to take advantage of these noncombinatorial entropy of mixing effects. Of course in reality most mixtures are not athermal and it is difficult, if not impossible, to change the polymer structure without also influencing the energetic interactions between chain segments and unfavorable compressibility effects.

The miscibility of most real polymer mixtures is controlled by both structural or athermal, as well as, energetic effects. In many cases a χ parameter of the form

$$\chi = A(\phi) + B(\phi)/T$$

can satisfactorily be used to fit experimental data. The leading term A would be expected to contain the athermal effects of the type discussed here. Thus we would predict A to be negative with an approximate linear composition dependence. It should be pointed out, however, that the theory presented in this paper assumes that mixing occurs at constant volume and, hence, there are no equation-of-state effects.[4b,c] These equation-of-state effects, which can be included within the context of our theory, will always destabilize the miscible mixture and can lead to LCST behavior.[4b,c] Thus A can be positive or negative depending on the relative importance of equation-of-state versus structural asymmetry effects.

In this paper we have studied the athermal blend in an attempt to isolate the effects of structure on the miscibility of polymer blends. The opposite case, the "isotopic blend" consisting of a mixture of structurally identical polymers with dissimilar attractive interactions, has also been studied.[18,19,32] The B term above will originate from these energetic effects and, in general, contains both enthalpic and noncombinatorial entropy contributions. The more general case in which both structural and energetic effects are present at the same time can be handled in a straightforward manner using the numerical techniques discussed earlier. One can anticipate that there may be cross terms in χ such that A and B can no longer be thought of as purely structural and purely energetic contributions. We are currently studying this general polymer blend.

Finally, it should be pointed out that, for the calculations presented in this investigation, we have ignored the intramolecular/intermolecular self-consistency problem by assuming that both types of chains in the mixture are ideal, Gaussian chains. We know, however, that the ideality approximation breaks down on sufficiently short length scales,[14] resulting in localized chain expansion ("localized stiffness"). As mentioned above, equation-of-state effects due to nonconstant volume of mixing are also not included in these calculations on athermal mixtures. While both of these important refinements to the model can and will be incorporated at a future date, we

anticipate that the qualitative effects we have demonstrated in this paper will be unchanged.

References and Notes

(1) Stein, R. S.; Murray, C. T.; Yang, H.; Soni, V.; Lo, R. J. *Physica B* **1986**, *137*, 194. Wignall, G. D. *Encycl. Polym. Sci. Eng.* **1987**, *10*, 112.
(2) Wignall, G. D.; Crist, B.; Russell, T. P.; Thomas, E. L. Scattering, Deformation, and Fracture in Polymers. *Proc. MRS Symp.* **1987**, 79.
(3) Flory, P. J. *Principles of Polymer Chemistry*; Cornell University, Ithaca, NY, 1953.
(4) For reviews see: (a) Paul, D. R.; Barlow, J. W. In *Polymer Compatibility and Incompatibility*; Solc, K., Ed.; MMI Press: Midland, MI, 1981; p 1. (b) Sanchez, I. C. *Polymer Compatibility and Incompatibility*; MMI Press: Midland, MI, 1981; p 59. (c) Sanchez, I. C. *Ann. Rev. Mater. Sci.* **1983**, *13*, 387.
(5) Bates, F. S.; Koehler, W. C.; Wignall, G. D.; Fetters, L. J. Reference 2, p 159.
(6) Ito, H.; Russell, T. P.; Wignall, G. D. *Macromolecules* **1987**, *20*, 2214.
(7) Yang, H.; O'Reilly, J. M. Reference 2, p 129.
(8) Trask, C. A.; Roland, C. M. *Macromolecules* **1989**, *22*, 256.
(9) Schweizer, K. S.; Curro, J. G. *Phys. Rev. Lett.* **1987**, *58*, 246.
(10) Curro, J. G.; Schweizer, K. S. *Macromolecules* **1987**, *20*, 1928.
(11) Curro, J. G.; Schweizer, K. S. *J. Chem. Phys.* **1987**, *87*, 1842.
(12) Schweizer, K. S.; Curro, J. G. *Macromolecules* **1988**, *21*, 3070.
(13) Schweizer, K. S.; Curro, J. G. *Macromolecules* **1988**, *21*, 3082.
(14) Curro, J. G.; Schweizer, K. S.; Grest, G. S.; Kremer, K. *J. Chem. Phys.* **1989**, *91*, 1357.
(15) Chandler, D.; Andersen, H. C. *J. Chem. Phys.* **1972**, *57*, 1930.
(16) Chandler, D. In *Studies in Statistical Mechanics*; Montroll, E. W., Lebowitz, J. L., Eds.; North-Holland: Amsterdam, 1982; Vol. VIII, p 274 and references cited therein.
(17) Schweizer, K. S.; Curro, J. G. *Phys. Rev. Lett.* **1988**, *60*, 809.
(18) Curro, J. G.; Schweizer, K. S. *J. Chem. Phys.* **1988**, *88*, 7242.
(19) Schweizer, K. S.; Curro, J. G. *J. Chem. Phys.* **1989**, *91*, 5059.
(20) Bawendi, M. G.; Freed, K. F. *J. Chem. Phys.* **1988**, *88*, 2741.
(21) Bawendi, M. G.; Freed, K. F.; Mohanty, U. *J. Chem. Phys.* **1987**, *87*, 5534.
(22) Freed, K. F.; Pesci, A. I. *J. Chem. Phys.* **1987**, *87*, 5534.
(23) Flory, P. J. *J. Chem. Phys.* **1949**, *17*, 203.
(24) de Gennes, P.-G. *Scaling Concepts in Polymer Physics*; Cornell University Press: Ithaca, NY, 1979.
(25) Lowden, L. J.; Chandler, D. *J. Chem. Phys.* **1974**, *61*, 5228; **1973**, *59*, 6587; **1975**, *62*, 4246.
(26) Henderson, D. *Ann. Rev. Phys. Chem.* **1974**, *25*, 461.
(27) Kac, M.; Uhlenbeck, G.; Hemmer, P. D. *J. Math. Phys.* **1963**, *4*, 216.
(28) Schweizer, K. S.; Curro, J. G., in preparation.
(29) Paluka, T.; Geyler, S. *Macromolecules* **1988**, *21*, 1665.
(30) Cates, M. E.; Deutsch, J. M. *J. Phys. (Les Ulis, Fr.)* **1986**, *47*, 2121.
(31) Brereton, M. G.; Fischer, E. W.; Herkt-Maetzky, C.; Mortensen, K. *J. Chem. Phys.* **1987**, *87*, 6144.
(32) Curro, J. G.; Schweizer, J. G., in preparation.

Registry No. PMMA, 9011-14-7; PEO, 25322-68-3.

Physical Aging in Poly(methyl methacrylate)/ Poly(styrene-*co*-acrylonitrile) Blends. 3. Simulation of Enthalpy Relaxation Using the Moynihan Model

Tai Ho and Jovan Mijović*

Department of Chemical Engineering, Polytechnic University, 333 Jay Street, Brooklyn, New York 11201.

Received August 7, 1989; Revised Manuscript Received September 12, 1989

ABSTRACT: The Moynihan model was used to simulate enthalpy relaxation of a series of blends of poly(methyl methacrylate) (PMMA) with poly(styrene-*co*-acrylonitrile) (SAN). The optimized Moynihan parameters for each blend composition were obtained from the best fits of specific heat data in the glass transition region measured in the rate-heating approach experiments, whereby samples were reheated immediately after being cooled through the glass transition region. Optimization was carried out by using the Marquardt algorithm. The optimized parameters were then used in simulations of experiments following the isothermal approach, in which a period of isothermal relaxation was introduced between cooling and heating steps. Calculated values for the isothermal enthalpy relaxation agreed with previously reported experimental data within the margins of experimental uncertainty. The discrete formulation of the Moynihan model was meticulously constructed to ensure an accurate representation of that model.

Introduction

In the past 3 decades, researchers have devoted much effort to studying relaxation of glasses in the region which encompasses the glass transition and extends well into the glassy state. In that region, a change in temperature or the application of a small external mechanical load will cause time-dependent changes, or relaxation, in the structure, with concurrent changes in the properties of the material. Relaxation that leads to changes in the structure is referred to as structural relaxation, while the effect of relaxation under stress on properties of materials is one of the topics of viscoelasticity.[1]

Structural relaxation in polymers has been studied by following either volume relaxation[2,3] or enthalpy relaxation.[4-10] In Kovacs' classic work,[2,3,11] volume relaxation in organic glasses was found to be characterized by nonlinearity and nonexponentiality. Since volume relaxation is one of the many manifestations of structural relaxation, those two characteristics should also mark the structural relaxation of glasses in general. Moreover, Struik[12] has recently demonstrated that creep compliance of glasses also exhibits those characteristics. In a previous communication from our laboratory,[13] we have shown that the enthalpy relaxation of blends of poly-

* To whom correspondence should be addressed.

0024-9297/90/2223-1411$02.50/0